Effect of Low - Intensity Focused Ultrasound on CaN and NFAT Expression Following Spinal Cord Injury in Rats

Zhuorui HE, Junjie CAI, Wanxin SUN, Chenyu ZHANG, Shupeng ZHU, Fanyi WU, Liqun REN*

Hebei Key Laboratory of Neural Injury and Repair, Chengde Medical University, Chengde 067000, China

Abstract [**Objectives**] To investigate the effect of low-intensity focused ultrasound (LIFU) on rats with spinal cord injury (SCI) by examining the expression of calcineurin (CaN) and nuclear factor of activated T-cells (NFAT) in the injured spinal cord region following LIFU intervention. [**Methods**] Twenty-four specific pathogen-free (SPF) female Wistar rats, aged 7 - 8 weeks (160 - 180 g), were selected. Six rats were randomly assigned to the sham-operated group (SHAM), undergoing laminectomy only without spinal cord injury. Spinal cord injury models were established in the remaining rats using a modified Allen's weight-drop method at the T10 thoracic vertebral level. The 18 rats with successful modeling were then randomly divided into the spinal cord injury model group (SCI group), LIFU treatment group 1 (T1 group), and LIFU treatment group 2 (T2 group), with six rats in each group. LIFU treatment (for T1 and T2 groups) commenced on day 4 after injury, administered once daily for 20 min per session, for a total of 11 consecutive days. Tissues were harvested on day 14. Changes in CaN and NFAT4 mRNA expression were assessed using quantitative polymerase chain reaction (qPCR). Changes in CaN and NFAT4 protein expression were evaluated by Western blot analysis. [**Results**] qPCR analysis revealed that compared to the SHAM group, mRNA expression levels of both CaN and NFAT4 were decreased in the SCI group; compared to the SCI group, mRNA expression levels of CaN and NFAT4 were increased in both the T1 and T2 groups; furthermore, compared to the T1 group, mRNA expression levels of CaN and NFAT4 were higher in the T2 group. Western Blot analysis showed that compared to the SHAM group, protein expression levels of both CaN and NFAT4 were downregulated in the SCI group; compared to the SCI group, protein expression levels of CaN and NFAT4 were increased in both the T1 and T2 groups; moreover, compared to the T1 group, protein expression levels of CaN and NFAT4 were higher in the T2 group. [**Conclusions**] LIFU may contribute to functional recovery in SCI rats by modulating the expression levels of CaN and NFAT4.

Key words Spinal cord injury, Low-intensity focused ultrasound, Calcineurin, Nuclear factor of activated T-cells

1 Introduction

Spinal cord injury (SCI) represents an extremely severe neurological disorder, with a reported global annual incidence ranging from 104 to 830 cases per 10 million population[1]. SCI can be categorized into primary injury and secondary injury[2]. Primary injury typically results from external mechanical impact, while secondary injury involves a cascade of inflammatory, edematous, ischemic, and oxidative stress responses that cause further damage to neural tissue following the primary insult[3-5].

Current clinical management of SCI primarily relies on surgical intervention and pharmacological therapies. However, these approaches often entail adverse effects and frequently yield suboptimal therapeutic outcomes. Consequently, neuromodulation techniques such as magnetic stimulation, electrical stimulation, and ultrasound stimulation have emerged as promising adjunctive therapies and are currently active areas of research[2]. Low-intensity focused ultrasound (LIFU) has garnered significant attention due to its non-invasive nature, high spatial resolution, and strong tissue penetration capabilities[6]. Studies have demonstrated that LIFU can modulate neuronal activity and stimulate the release of neurotrophic factors, thereby facilitating neural repair[6-7].

Calcineurin (CaN) is a calcium/calmodulin-dependent serine/threonine protein phosphatase, composed of a catalytic subunit A and a regulatory subunit B, forming a heterodimer[8]. Highly expressed in neurons, CaN is directly activated by calcium ions (Ca^{2+}) and plays a crucial role in numerous Ca^{2+}-dependent signal transduction pathways[9-10].

The nuclear factor of activated T-cells (NFAT) family comprises five members: NFATc1, NFATc2, NFATc3, NFATc4, and NFAT5[11]. The activity of NFATc1-c4 is regulated by the Ca^{2+}/calcineurin signaling pathway. Under resting conditions, they reside in the cytoplasm in a highly phosphorylated state. Upon elevation of intracellular Ca^{2+} and subsequent activation of CaN, NFATc1-c4 are dephosphorylated and rapidly translocate into the nucleus, where they initiate the transcription of downstream target genes. In contrast, NFAT5 is primarily activated by osmotic stress[12]. NFAT participates extensively in physiological processes across multiple systems, including the nervous, cardiac, and skeletal systems[13]. Research indicates that NFAT signaling plays multifaceted roles in neural development, axonal regeneration, and synaptic plasticity[14]. Existing studies suggest that LIFU may activate mechanosensitive ion channels, leading to increased intracellular Ca^{2+} levels, which in turn could mediate neuroprotection and axonal regeneration via the CaN-NFAT pathway; however, the precise mechanism remains incompletely understood[14]. This study aimed to investigate the impact of LIFU stimulation on rats with SCI by examining the expression of CaN and NFAT.

2 Materials and methods

2.1 Experimental animals and grouping Twenty-four adult female Wistar rats of specific pathogen-free (SPF) grade, aged

Received: August 13, 2025 Accepted: November 26, 2025

Supported by 2025 Yanzhao Youzhou Tower Talent Gathering Program—Elite Talent Project (Overseas Platform) Foreign Expert Category.

Zhuorui HE, master's degree. * Corresponding author. Liqun REN, doctoral degree, professor.

6 – 8 weeks (200 ± 20 g), were supplied by Beijing Vital River Laboratory Animal Technology Co., Ltd. [Animal Qualification Certificate No. SCXK (Beijing) 2021-0006]. They were housed in the Experimental Animal Center of Chengde Medical University [License No. SYXK (Hebei) 2022-002], under controlled conditions: ambient temperature 22 – 23 ℃, relative humidity 60% – 70%, and a 12-h light/dark cycle. All experimental procedures were approved by the Animal Ethics Committee of Chengde Medical University (Approval No. CDMULAC-20240628-029). Following a one-week acclimatization period, six rats were randomly selected using a random number table to serve as the sham-operated group (SHAM). Spinal cord injury was induced in the remaining 18 rats at the T10 thoracic vertebral level using a modified Allen's weight-drop method. The 18 rats with successful modeling were then randomly divided into three groups ($n = 6$ per group): the spinal cord injury model group (SCI group), LIFU treatment group 1 (T1 group), and LIFU treatment group 2 (T2 group).

2.2 Main instruments and reagents Animal Anesthesia Machine (RWD Life Science Co., Ltd., Shenzhen, China), Brain Stereotaxic Apparatus (RWD Life Science Co., Ltd., Shenzhen, China), Spinal Cord Impactor (RWD Life Science Co., Ltd., Shenzhen, China), Low-Intensity Focused Ultrasound Stimulator (Puzhuo, Jiangxi, China).

BCA Protein Assay Kit, High – Efficiency RIPA Tissue Rapid Lysis Buffer, Skim Milk Powder, PMSF (Beijing Solarbio Science & Technology Co., Ltd.), PAGE Gel Fast Preparation Kit (Yeasen Biotechnology, Shanghai, China), Protease Inhibitor Cocktail (Roche Diagnostics, Basel, Switzerland), GAPDH Antibody (Cell Signaling Technology, Danvers, MA, USA), CaN Antibody (Abways Technology, Shanghai, China), NFAT4 Antibody (Thermo Fisher Scientific, Waltham, MA, USA), TRIzol® Reagent (Invitrogen, Thermo Fisher Scientific, Waltham, MA, USA), Real – Time Quantitative PCR (qPCR) Reagent Kit, and Reverse Transcription Reagent Kit (Takara Bio, Kusatsu, Shiga, Japan).

2.3 SCI model preparation Rats were anesthetized via intraperitoneal injection. After fur removal, the rats were secured on the surgical table. The skin and muscles were incised using a scalpel. The T10 spinous process was identified. The T10 thoracic vertebra was removed using bone rongeurs to expose the spinal cord. For the model groups, a modified Allen's weight-drop method was employed, where a 10 g weight was dropped vertically from a height of 6 cm onto the exposed spinal cord. Successful model establishment was confirmed by the presence of localized swelling and hemorrhage at the impact site, accompanied by tail flicking and hindlimb spasms post-impact. The SHAM group underwent laminectomy only, without spinal cord injury induction. Following successful model establishment, SCI rats received bladder massage twice daily (morning and evening) to assist in urination. The urethral area was disinfected with iodophor, and penicillin (160 000 U/day) was administered intraperitoneally for 3 consecutive days.

2.4 LIFU treatment Rats were anesthetized and immobilized in a brain stereotaxic apparatus. The ultrasound transducer was positioned over the dorsal surface corresponding to the T12 spinal segment. Ultrasound gel was applied to fill the space between the skin and the transducer, ensuring the absence of air bubbles. Stimulation parameters for the T1 group: acoustic pressure = 0.64 MPa, duty cycle = 50%. Stimulation parameters for the T2 group: acoustic pressure = 0.96 MPa, duty cycle = 50%. Treatment was administered once daily for 20 minutes per session, over a period of 11 consecutive days.

2.5 Sample processing and collection Tissue harvesting was performed after 11 consecutive days of treatment. Under anesthesia, a segment of spinal cord tissue approximately 1 cm long, centered on the injury site, was excised and placed into a microcentrifuge tube. Samples were stored at −80 ℃ for subsequent qPCR and Western blot analyses.

2.6 Reverse Transcription Quantitative Polymerase Chain Reaction (RT-qPCR) Approximately 50 mg of spinal cord tissue was homogenized in 1 mL of TRIzol reagent and incubated at room temperature for 5 min. Subsequently, 0.2 mL of chloroform was added, followed by vigorous shaking for 15 seconds and incubation at room temperature for 3 min. The mixture was centrifuged at 12 000 rpm for 15 min; the aqueous phase (upper layer) was then transferred to a new microcentrifuge tube. Isopropanol (0.2 mL) was added to the aqueous phase, mixed, and incubated at room temperature for 10 min. The sample was centrifuged at 12 000 rpm for 10 min, and the supernatant was discarded. The RNA pellet was washed by adding 1 mL of 75% ethanol, followed by centrifugation at 8 000 rpm for 5 min (repeated twice), and the supernatant was discarded after each wash. The RNA pellet was air-dried at room temperature for 10 min to ensure complete ethanol evaporation. The dried RNA pellet was dissolved in DEPC-treated water, and the RNA concentration and purity were measured. Reverse transcription was performed using the TaKaRa PrimeScript RT Reagent Kit (see Table 1 for primers), and the resulting cDNA was stored at −80 ℃. Quantitative PCR amplification was subsequently carried out using cDNA as the template.

Table 1 Primer sequences

Target gene	Forward sequence	Reverse sequence	Product size//bp
CaN	GAAAGCCGTTCCATTTCCGC	TTTCTTCCAGCCTGCCTTCC	122
NFAT	CTCATTGGGAGGCTGAAGGAA	CTTGCTTCATCAAAACTGGTGT	189
GAPDH	AGGTCGGTGTGAACGGATTTG	TGTAGACCATGTAGTTGAGGTCA	183

2.7 Western Blot analysis of CaN and NFAT4 protein expression Spinal cord tissue was weighed and placed into sterile, nuclease-free microcentrifuge tubes. Lysis working buffer (10 times the tissue weight) was added to each tube. This buffer was pre-

pared by mixing High – Efficiency RIPA Lysis Buffer, PMSF, and Protease Inhibitor Cocktail in a 50 ∶ 1 ∶ 4 ratio. Tissues were homogenized in a tissue grinder at 50 Hz for 30 sec; this cycle was repeated 6 times. The resulting homogenate was centrifuged at 4 ℃ and 12 000 rpm for 15 min. The supernatant, containing the total protein extract, was carefully transferred to a new microcentrifuge tube. Protein concentration was determined using the BCA protein assay kit. Loading buffer (added at one-fourth of the total volume) was mixed with the protein samples, followed by boiling for denaturation. Samples were then subjected to sodium dodecyl sulfate-polyacrylamide gel electrophoresis (SDS-PAGE), followed by transfer onto polyvinylidene difluoride (PVDF) membranes and blocking. Membranes were incubated overnight at 4 ℃ with primary antibodies: anti-CaN (1 ∶ 1 000 dilution), anti-NFAT4 (1 ∶ 1 000 dilution), and anti-GAPDH (1 ∶ 6 000 dilution). The following day, membranes were washed four times and incubated with horseradish peroxidase (HRP)-conjugated secondary antibody (1 ∶ 10 000 dilution) at room temperature for 1 h. After three additional washes, enhanced chemiluminescence (ECL) substrate was applied to the membranes. Protein bands were visualized using a chemiluminescence imaging system. Band intensity (gray value) was quantified using ImageJ software. The relative expression level of each target protein was calculated as the ratio of its band intensity to that of the internal control (GAPDH).

2.8 Statistical analysis Data were processed using GraphPad Prism version 10 and SPSS Statistics version 25 software. Continuous data are presented as mean ± standard deviation ($\bar{x} \pm s$). All measurement data conformed to a normal distribution. Intergroup comparisons were performed using one-way analysis of variance (ANOVA). If the assumption of homogeneity of variance was met, post-hoc pairwise comparisons were conducted using Fisher's Least Significant Difference (*LSD*) test. If the assumption of homogeneity of variance was violated, Tamhane's T2 test was used for pairwise comparisons. A *p*-value less than 0.05 ($P<0.05$) was considered statistically significant.

3 Results and analysis

3.1 RT-qPCR results Bar graphs depicting the relative mRNA expression levels of CaN and NFAT4 across the experimental groups are shown in Fig. 1. Results demonstrated that compared to the SHAM group, mRNA expression levels of both CaN and NFAT4 were significantly downregulated in the SCI group ($P<0.001$); compared to the SCI group, mRNA expression levels of CaN and NFAT4 were significantly increased in the T2 group ($P<0.001$ for CaN, $P<0.05$ for NFAT4). Furthermore, mRNA expression levels of CaN and NFAT4 were significantly higher in the T2 group compared to the T1 group ($P<0.001$ for CaN, $P<0.05$ for NFAT4).

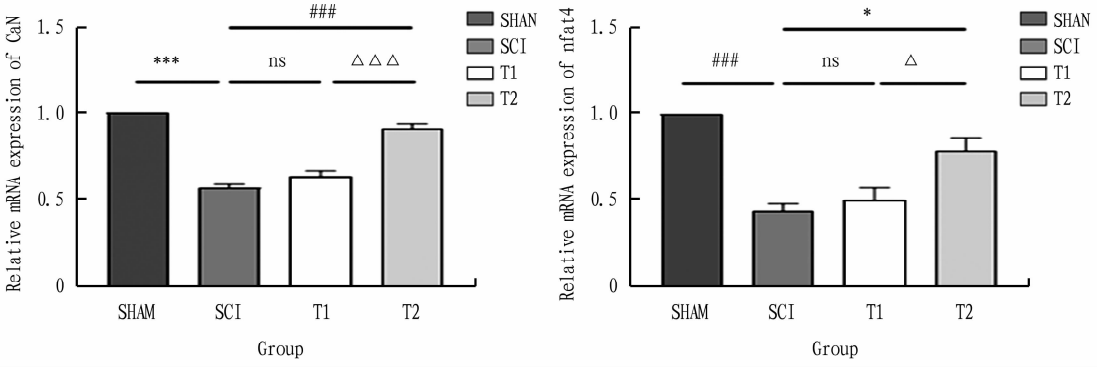

NOTE Compared with SHAM group: $^{###}P<0.001$; compared with SCI group: $^{***}P<0.001$, $^{*}P<0.05$; $^{ns}P>0.05$; compared with T1 group: $^{△△△}P<0.001$, $^{△}P<0.05$.

Fig. 1 Comparison of CaN and NFAT4 mRNA expression levels among groups in rats

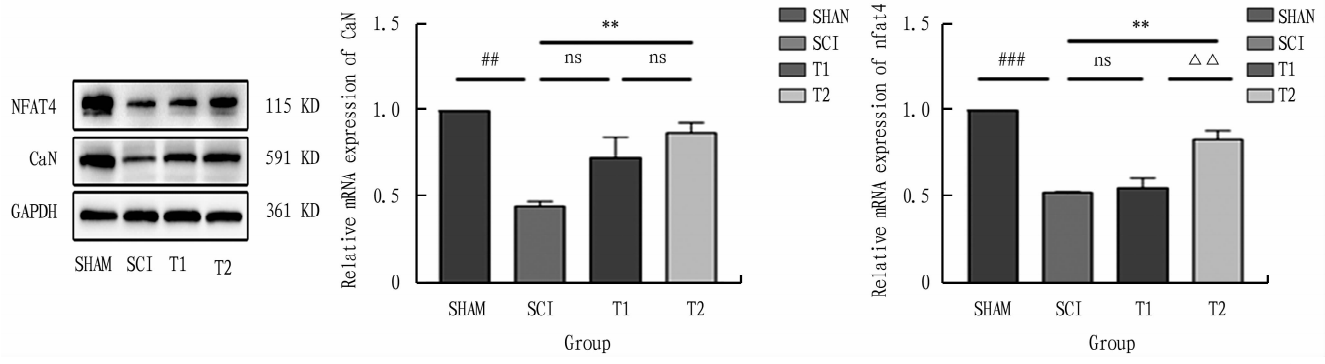

NOTE Compared with SHAM group: $^{##}P<0.01$, $^{###}P<0.001$; compared with SCI group: $^{**}P<0.01$; $^{ns}P>0.05$; compared with T1 group: $^{△△}P<0.01$, $^{ns}P>0.05$.

Fig. 2 Protein expression levels of CaN and NFAT4 among groups in rats

3.2 Western Blot results Bar graphs illustrating the relative protein expression levels of CaN and NFAT4 across the experimental groups are presented in Fig. 2. Results indicated that compared to the SHAM group, protein expression levels of CaN and NFAT4 were significantly downregulated in the SCI group ($P < 0.01$ for CaN, $P < 0.001$ for NFAT4); compared to the SCI group, protein expression levels of both CaN and NFAT4 were significantly increased in the T2 group ($P < 0.01$); moreover, NFAT4 protein expression was significantly higher in the T2 group compared to the T1 group ($P < 0.01$).

4 Discussion

SCI is a complex and devastating disorder of the central nervous system. Secondary injury, initiated within minutes of the primary insult, represents a dynamic process that evolves over weeks to months. Characterized by pathological features such as inflammation, oxidative stress, cellular edema, and ionic dyshomeostasis, secondary injury exacerbates irreversible tissue damage[15-16]. Current therapeutic strategies primarily aim to mitigate the progression of inflammation, edema, and oxidative stress induced by secondary injury, while maximizing the preservation of structure and function in surviving neurons[17].

LIFU has been shown to attenuate inflammation, reduce reactive oxygen species (ROS) production and oxidative stress, and promote the release of neurotrophic factors, thereby facilitating neural repair[7,18]. The activity of CaN is regulated by intracellular Ca^{2+} concentration. NFAT (specifically NFATc1-c4) represents its most extensively studied downstream effector. The CaN-NFAT signaling pathway plays crucial regulatory roles in diverse physiological processes, including myelination, synaptogenesis, learning, and memory[9]. Studies indicate that activating this pathway enhances cellular proliferation and differentiation capacity, thereby accelerating tissue repair[19]; in diabetic rat wound models, activation of the CaN-NFAT pathway similarly shortens healing time, attributed to enhanced cellular proliferation[20]. Research has demonstrated that ultrasound stimulation can significantly promote NFAT nuclear translocation and enhance its transcriptional activity[14]. Therefore, we hypothesized that LIFU might promote spinal cord injury recovery by activating the CaN-NFAT signaling pathway. Our findings revealed that compared to the SCI group, protein expression of both CaN and NFAT4 was significantly upregulated in the T2 treatment group ($P < 0.05$). While the T1 group showed an increasing trend in CaN and NFAT4 protein expression compared to the SCI group, this difference did not reach statistical significance. The differential therapeutic outcomes between the T1 and T2 groups indicate that the selection of LIFU parameters significantly influences efficacy. The higher acoustic pressure used in the T2 group (0.96 MPa) yielded superior therapeutic effects compared to the lower pressure used in the T1 group (0.64 MPa). These results suggest that the neuroprotective mechanism of LIFU may involve elevating intracellular Ca^{2+} levels, thereby activating the CaN-NFAT signaling pathway: LIFU stimulation likely induces transient Ca^{2+} influx, rapidly elevating cytosolic Ca^{2+} concentration; elevated Ca^{2+} activates CaN, leading to dephosphorylation of the downstream transcription factor NFAT, exposure of its nuclear localization signal, translocation into the nucleus, and initiation of target gene transcription by nuclear NFAT.

This study demonstrates that LIFU exerts neuroprotective effects in the treatment of SCI. Its mechanism appears to be associated with the CaN-NFAT signaling pathway. Further validation of CaN enzymatic activity, NFAT nuclear translocation, and downstream target gene expression is warranted to confirm the genuine activation of this pathway.

References

[1] KAKA GR, MODARRESI F. Conditioned medium derived from mesenchymal stem cells and spinal cord injury: A review of the current therapeutic capacities[J]. IBRO Neuroscience Reports, 2025.

[2] HU X, XU W, REN Y, *et al.* Spinal cord injury: Molecular mechanisms and therapeutic interventions[J]. Signal Transduction and Targeted Therapy, 2023, 8(1): 245.

[3] STERNER RC, STERNER RM. Immune response following traumatic spinal cord injury: Pathophysiology and therapies[J]. Frontiers in Immunology, 2023, 13: 1084101.

[4] MA H, WANG C, HAN L, *et al.* Tofacitinib promotes functional recovery after spinal cord injury by regulating microglial polarization via JAK/STAT signaling pathway[J]. International Journal of Biological Sciences, 2023, 19(15): 4865.

[5] ZHONG M, FAN G, AN Z, *et al.* Research progress on long non-coding RNAs for spinal cord injury[J]. Journal of Orthopaedic Surgery and Research, 2023, 18(1): 520.

[6] XU T, LU X, PENG D, *et al.* Ultrasonic stimulation of the brain to enhance the release of dopamine: A potential novel treatment for Parkinson's disease[J]. Ultrasonics Sonochemistry, 2020, 63: 104955.

[7] ZHONG YX, LIAO JC, LIU X, *et al.* Low intensity focused ultrasound: A new prospect for the treatment of Parkinson's disease[J]. Annals of Medicine, 2023, 55(2): 2251145.

[8] RUSNAK F, MERTZ P. Calcineurin: Form and function[J]. Physiological Reviews, 2000, 80(4): 1483-1521.

[9] KIPANYULA MJ, KIMARO WH, ETET PFS. The emerging roles of the calcineurin-nuclear factor of activated T-lymphocytes pathway in nervous system functions and diseases[J]. Journal of Aging Research, 2016, 2016(1): 5081021.

[10] ULENGIN-TALKISH I, CYERT MS. A cellular atlas of calcineurin signaling[J]. Biochimica et Biophysica Acta (BBA)-Molecular Cell Research, 2023, 1870(1): 119366.

[11] MACKIEWICZ J, LISEK M, BOCZEK T. Targeting CaN/NFAT in Alzheimer's brain degeneration[J]. Frontiers in Immunology, 2023, 14: 1281882.

[12] KITAMURA N, KAMINUMA O. Isoform-selective NFAT inhibitor: Potential usefulness and development[J]. International Journal of Molecular Sciences, 2021, 22(5): 2725.

[13] LIN Y, SONG Y, ZHANG Y, *et al.* NFAT signaling dysregulation in cancer: Emerging roles in cancer stem cells[J]. Biomedicine & Pharmacotherapy, 2023, 165: 115167.

[14] TRUONG TT, CHIU WT, LAI YS, *et al.* Ca^{2+} signaling-mediated low-intensity pulsed ultrasound-induced proliferation and activation of motor neuron cells[J]. Ultrasonics, 2022, 124: 106739.
[15] HWANG BY, MAMPRE D, AHMED AK, *et al.* Ultrasound in traumatic spinal cord injury: A wide-open field[J]. Neurosurgery, 2021, 89(3): 372-382.
[16] DING Y, CHEN Q. Recent advances on signaling pathways and their inhibitors in spinal cord injury[J]. Biomedicine & Pharmacotherapy, 2024, 176: 116938.
[17] HILTON BJ, MOULSON AJ, TETZLAFF W. Neuroprotection and secondary damage following spinal cord injury: Concepts and methods[J]. Neuroscience Letters, 2017, 652: 3-10.
[18] LIAO YH, CHEN MX, CHEN SC, *et al.* Low-intensity focused ultrasound alleviates spasticity and increases expression of the neuronal K-Cl cotransporter in the L4-L5 sections of rats following spinal cord injury[J]. Frontiers in Cellular Neuroscience, 2022, 16: 882127.
[19] SHEN XX. The study on the effect and mechanism of the PBM-activited Ca^{2+}/NFAT on the proliferation and differentiation of ESCs and wound healing[D]. Chongqing: Army Medical University of PLA, 2021. (in Chinese).
[20] GE XY. Effects of MEBT/MEBO on expression of CaN/NFAT signaling pathway in wound surface of diabetic rats[D]. Baise: Youjiang Medical University for Nationalities, 2024. (in Chinese).

(From page 68)

[21] PAOLUCCI S, ANTONUCCI G, GRASSO MG, *et al.* Early versus delayed inpatient stroke rehabilitation: A matched comparison conducted in Italy[J]. Archives of Physical Medicine and Rehabilitation, 2000, 81(6): 695-700.
[22] IYER MB, SCHLEPER N, WASSERMANN EM. Priming stimulation enhances the depressant effect of low-frequency repetitive transcranial magnetic stimulation[J]. Journal of Neuroscience, 2003, 23(34): 10867-10872.
[23] NORDMANN G, AZORINA V, LANGGUTH B, *et al.* A systematic review of non-motor rTMS induced motor cortex plasticity[J]. Frontiers in Human Neuroscience, 2015, 9: 416.
[24] XU J, BRANSCHEIDT M, SCHAMBRA H, *et al.* Rethinking interhemispheric imbalance as a target for stroke neurorehabilitation[J]. Annals of Neurology, 2019, 85(4): 502-513.
[25] BÜTEFISCH CM, WESSLING M, NETZ J, *et al.* Relationship between interhemispheric inhibition and motor cortex excitability in subacute stroke patients[J]. Neurorehabilitation and Neural Repair, 2008, 22(1): 4-21.
[26] GUO Z, JIN Y, BAI X, *et al.* Distinction of high- and low-frequency repetitive transcranial magnetic stimulation on the functional reorganization of the motor network in stroke patients[J]. Neural Plasticity, 2021, 2021: 8873221.

(From page 74)

[2] POWELL K, LEROUX E, BANKS JP, *et al.* Developing a written action plan for children with eczema: A qualitative study[J]. British Journal of General Practice, 2018, 68(667): e81-e89.
[3] MASLIN D, VEITCH D, WILLIAMS HC. Direct infant ultraviolet light exposure is associated with eczema and immune development: A critical appraisal[J]. British Journal of Dermatology, 2020, 182(2): 300-303.
[4] CHEN SX, DU X, JING HX, *et al.* Observation on the efficacy of chloramphenicol and prednisone liniment in the treatment of acute eczema[J]. Dermatology and Venereology, 2019, 41(2): 239-241. (in Chinese).
[5] Professional Committee of Experimental Pharmacology of Chinese Materia Medica, China Association of Chinese Medicine. Specifications for preparation of eczema models (draft)[J]. Chinese Journal of Experimental Traditional Medical Formulae, 2017, 23(24): 6-10. (in Chinese).
[6] CHEN SX, DU X, JING HX, *et al.* Experimental study on anti-inflammatory, anti-allergic and anti-pruritic effects of chloramphenicol prednisone liniment in animals[J]. Journal of Pediatric Pharmacy, 2020, 26(12): 1-3. (in Chinese).
[7] DAI YQ, DU CM, XIE HP, *et al.* Intervention effect of Huangbai capsule combined with olotatidine hydrochloride on acute eczema model rats and its anti-allergic mechanism[J]. Modern Journal of Integrated Traditional Chinese and Western Medicine, 2021, 30(9): 926-930, 1005. (in Chinese).
[8] POWELL K, LEROUX E, BANKS JP, *et al.* Developing a written action plan for children with eczema:A qualitative study[J]. British Journal of General Practice, 2018, 68(667): e81-e89.
[9] ZHANG LL, WANG J, JIANG T, *et al.* Antipruritic and anti-allergic effects of the active fraction from dryopteris fragrans[J]. Chinese Traditional Patent Medicine, 2016, 38(11): 2476-2480. (in Chinese).
[10] ZHANG JZ. Classification of glucocorticoid and clinical use in dermatology[J]. China Medical Abstracts: Dermatology, 2015, 32(3): 241-247. (in Chinese).
[11] ZHAN M, ZHENG W, JIANG Q, *et al.* Upregulated expression of substance P (SP) and NK1R in eczema and SP-induced mast cell accumulation[J]. Cell Biology and Toxicology, 2017, 33(4): 389-405.
[12] XU W, HAO TT, LI J, *et al.* Mast cell activation related molecules and antibodies in differentiating allergic skin diseases[J]. Laboratory Medicine, 2016, 36(12): 1036-1039. (in Chinese).
[13] SONG XZ, SONG WM, XU AE, *et al.* Effects of aquaporin 3, Caspase 14 and bleomycin hydrolase on skin barrier function in chronic eczema[J]. Chinese Journal of Dermatology, 2012, 45(2): 83-86. (in Chinese).